Geomechanics and Engineering, *Vol. 20, No. 5 (2020) 421-432*
DOI: https://doi.org/10.12989/gae.2020.20.5.421

Complex analysis of rock cutting with consideration of rock-tool interaction using distinct element method (DEM)

Guangzhe Zhang[1a], Wengang Dang*[2,3,4], Martin Herbst[1a] and Zhengyang Song[1a]

[1]*Geotechnical Institute, TU Bergakademie Freiberg, Gustav-Zeuner-Str. 1, 09599 Freiberg, Germany*
[2]*School of Civil Engineering, Sun Yat-sen University, Gungzhou 520275, China*
[3]*Key Laboratory of Marine Civil Engineering of Guangdong, Guangzhou, 510006, China*
[4]*Southern Marine Science and Engineering Guangdong Laboratory, Zhuhai, 519082 China*

(Received October 28, 2019, Revised February 1, 2020, Accepted February 7, 2020)

Abstract. Cutting of rocks is very common encountered in tunneling and mining during underground excavations. A deep understanding of rock-tool interaction can promote industrial applications significantly. In this paper, a distinct element method based approach, PFC[3D], is adopted to simulate the rock cutting under different operation conditions (cutting velocity, depth of cut and rake angle) and with various tool geometries (tip angle, tip wear and tip shape). Simulation results showed that the cutting force and accumulated number of cracks increase with increasing cutting velocity, cut depth, tip angle and pick abrasion. The number of cracks and cutting force decrease with increasing negative rake angle and increase with increasing positive rake angle. The numerical approach can offer a better insight into the rock-tool interaction during the rock cutting process. The proposed numerical method can be used to assess the rock cuttability, to estimate the cutting performance, and to design the cutter head.

Keywords: crack pattern; cutting force; rake angle; rock-tool interaction; sandstone; tip abrasion

1. Introduction

In rock and mining engineering, conical picks assembled on roadheaders, miners and shearers are the essential cutting tools used to excavate hard rocks or coal (Wang *et al.* 2020). It is necessary to understand the cutting behavior in rock fragmentation in order to evaluate the cutting efficiency of the cutting tool and to predict his lifetime. For this propose, rock cutting experiments including in-situ, full-scale and small-scale tests have been carried out to determine the two in the rock cutting meaningful parameters, i.e., cutting force and specific energy, which can be used to estimate the performance of the rock cutting process and their affecting factors (Evans 1984, Cundall 1988, Yang *et al*. 2013, Ding *et al.* 2014, Chang *et al*. 2017, Zhu *et al*. 2017, Jeong and Jeon 2018, Shang *et al*. 2018). McFeat-Smith and Fowell (1977) estimated the performance of a roadheader from specific energy by conducting a series of in-situ rock cutting tests. They found that the cutting rate increases with decreasing specific energy. Hurt and MacAndrew (1985) studied the type and quality of the cutter head affecting the pick lifetime. They concluded that the design of cutter heads has a major impact on the pick consumption. Fowell *et al.* (1994) performed a scale-one cutting tests on a number of rock or rock-like materials like sandstone, coal, salt and concrete to predict the applied tool force and consumed specific energy under different cutting velocities and advance revolutions. They related the cutting performance to the rock strength properties. A decreasing trend of the cutting rate with increased compressive strength was found. Bilgin *et al.* (2006) conducted scale-one cutting tests with conical picks under different cutting conditions and correlated the cutting force and specific energy with rock strength properties including compressive strength, tensile strength and Young's modulus. It was found that both, the force and energy values, increase with increasing rock strength. Balci and Bilgin (2007) performed both, the full-scale and small-scale rock cutting tests and established a relationship with respect to the specific energy between the two experiments. They stated: the specific energy obtained from the small-scale test can be used as a guide to estimate the cutting rate of excavating machines.

Since in-situ and scale-one rock cutting experiments are usually cost expensive and time-consuming, and sometimes it is not easy to gain a large rock sample for the test, numerical approach is proposed to simulate the rock cutting process under different operating conditions. Another advantage of the numerical modelling is that the damage process or material removal process during the rock cutting can be analyzed, while experimental investigations cannot provide so much information about the crack initiation and propagation beneath the rock surface. The study of crack formation is meaningful for the design of an effective cutter head.

With the development of computer technology, numerical simulations of rock cutting have been conducted by using various modelling techniques, such as boundary

*Corresponding author, Associate Professor
E-mail: dangwg@mail.sysu.edu.cn
[a]Ph.D.

ISSN: 2005-307X (Print), 2092-6219 (Online)

element method (BEM), distinct element method (DEM), finite difference method (FDM) and finite element method (FEM). Among these, the DEM is widely used and which provides a better understanding of the mechanical behavior of rocks and rock masses (Kwok *et al.*, 2019; Shang *et al.*, 2019; Shang, 2020). It has been proven as an efficient and economical method to give a useful insight into rock fragmentation and fracture formation under complex load conditions.

The DEM was firstly proposed to model the mechanical behavior of rocks by Cundall (1971). A detailed description of this method is given by Cundall (1988) and Hart *et al.* (1988). According to the original definition (Cundall and Hart 1992), the DEM is a modelling technique that allows finite displacements and rotations of discrete bodies including complete detachment and automatic recognition of new contacts during the simulation progress. A particular instance of DEM is a particle based model, which can model the mechanical behavior of a system composed of an assembly of discrete spherical particles. The particles can move independently of one another and interact at pair-wise contacts. The particles are assumed to be rigid. The mechanical behavior of such a system is described in terms of the movement of each particle and the inter-particle forces acting at each contact point.

During the past few years, numerical simulations of rock cutting using DEM have also been conducted by many researchers. For example, Lei and Kaitkay (2003) developed a methodology to apply hydrostatic pressure on a sample surface for the rock cutting simulation using a 2D approach and studied the influence of some simulation condition-based parameters on the resulting cutting force. Su and Akcin (2011) extended 2D simulations of rock cutting towards 3D and established a relationship of cutting forces between numerical, experimental and theoretical results. Rojek *et al.* (2011) conducted the DEM simulation of rock cutting subjected to a conical pick to study the rock fragmentation and its relation to applied cutting force in both, 2D and 3D. Lunow and Konietzky (2012) used two different DEM-based codes to simulate the rock indenting and cutting by specifying different cutting parameters, such as indentation and cut depth, shape and tip angle of cutter head and rake angle between the tool and rock. Huang *et al.* (2013) discussed the ductile and brittle failure modes during rock cutting, which is dependent on the depth of cut, using 2D models. Van Wyk *et al.* (2014) performed simulations of the rock cutting process with two different cutting tools (chisel- and button-shaped), and investigated the influence of particle size on the resultant tool forces using 3D models.

The cutting parameters and the tool geometry affect the cutting forces and crack patterns significantly in rock cutting engineering (Li *et al*. 2019). It is important to select a correct cutter head which is appropriate and sufficient for cutting rocks with a higher cutting rate and a lower wear rate. This so-called 'trial-and-error' tests can be fulfilled by doing numerical simulations. In addition, a numerical approach can be used as a parametric study to estimate the rock cuttability, to evaluate the cutting performance and to design the cutter head. It can reduce much of the time-consuming and expensive experimental works. In this paper, numerical simulations of rock cutting with respect to a sandstone sample are conducted using the DEM-based code of PFC^{3D} (Itasca 2016) under different operating conditions to investigate the influence of cutting parameters including cutting velocity, depth of cut and rake angle, and tool geometry like tip angle, tip wear and tip shape on the resulting cutting force and crack pattern.

2. Numerical simulation of rock cutting

2.1 Model construction and calibration

Fig. 1 illustrates the thin section image of sandstone taken from Saxony of Germany. This sandstone is fine- to medium-grained with grain size ranging from 0.05-0.15 mm. The grain rounding varies from sub- to well-rounded, the grain sorting is between well- and moderately-sorted, and the grain bonding is exhibited predominantly by a direct grain-grain contact. Therefore, it can be regarded as a homogeneous and isotropic rock. The density and porosity of sandstone are 2060.8 kg/m^3 and 2.1%, respectively. According to the X-Ray diffraction analysis, the sandstone is consists of quartz (99.1%) and Kaolinite (0.9%). With respect to the mechanical properties, the sandstone has a uniaxial compressive strength (UCS) of 53.5 MPa, a Young's modulus of 17.5 GPa, a Poisson's ratio of 0.2 and a Brazilian tensile strength (BTS) of 4.6 MPa.

A deficiency by using the DEM is that the input micro-parameters cannot be derived from the laboratory experiments directly. The macro-parameters must be calibrated by simulating the rock mechanical experiments. Within this paper, numerical modellings are conducted by applying the particle code PFC^{3D} (Itasca, 2016), in which the bonded particle model associated with parallel bonds is used. The generation of particles and contacts is according to Potyondy and Cundall (2004). The micro-parameters are calibrated by simulating both, UCS and BTS tests. Fig. 2(a) illustrates a cylindrical model with 50 mm in diameter and 100 mm in height constructed for the simulation of the UCS test, and Fig. 2(b) illustrates the disc model (50 mm in diameter and 25 mm in thickness) for the BTS simulation. Since sandstone can be referred to as a mono-mineral and homogeneous rock, considering with the capacity of the PC, the ball radii are set to 0.4 - 0.6 mm. The resulting sample piece for the UCS test is composed of 357 982 balls. The UCS simulation is progressed by moving the top and bottom loading-walls compressing the particle assembly.

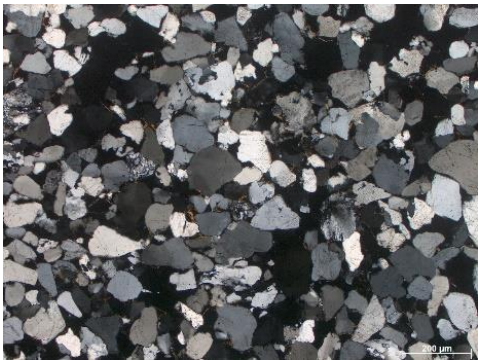

Fig. 1 Thin section image of Postaer sandstone

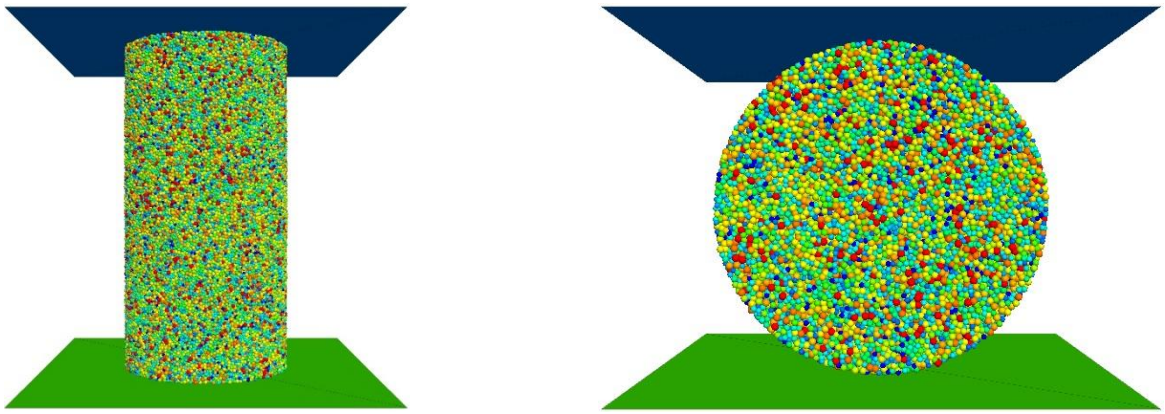

(a) (b)

Fig. 2 PFC models for the simulation of (a) UCS and (b) BTS tests

Table 1 Micro-parameters calibrated for sandstone

Component	Micro-parameter	Value
Particle (grain)	Density (ρ) [kg/m^3]	2060
	Minimum radius (r_{min}) [mm]	0.4
	Maximum radius (r_{max}) [mm]	0.6
	Effective modulus (E) [GPa]	8.2
	Normal-to-shear stiffness ratio (k = kn/ks) [-]	2.5
	Friction coefficient (μ) [-]	0.5
	Damping coefficient [-]	0.1
Parallel bond contact (Cement)	Effective modulus (E*) [GPa]	8.2
	Normal-to-shear stiffness ratio (k* = kn*/ks*) [-]	2.5
	Tensile strength (σ_t) [MPa]	13
	Cohesion (c) [MPa]	13
	Friction angle (φ) [°]	0

Table 2 Comparison of macro-properties between laboratory experiment and numerical simulation for sandstone

Macro-property	Experiment	Simulation	Deviation
Uniaxial compressive strength (UCS) [MPa]	53.5	53.4	0.2%
Young's modulus [GPa]	17.5	15.6	10.9%
Poisson's ratio [-]	0.2	0.21	5.0%
Brazilian tensile strength (BTS) [MPa]	4.6	5.1	10.9%

The velocity of the loading-walls is set to 0.05 m/s. The particle assembly is made of 91 525 balls for the BTS test, and the compressing velocities of loading-walls on the particle assembly are set to 0.02 m/s.

The calibration results of micro-parameters are summarized in Table 1. The macro-properties between experimental and numerical studies are compared in Table 2. As can be seen, the numerically obtained parameters (UCS, Young's modulus, Poisson's ratio and BTS) show a good agreement with those measured in the laboratory. It can be concluded that the micro-parameters calibrated for the sandstone model are valid and reliable.

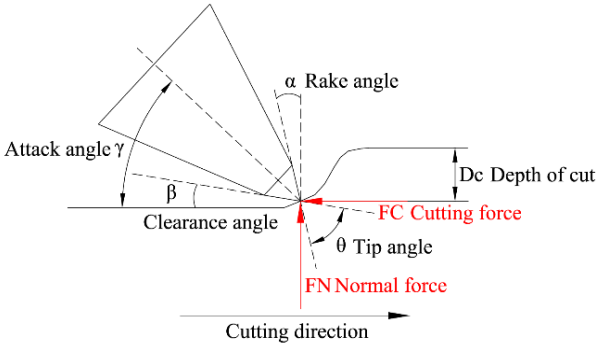

Fig. 3 Definition of cutting parameters for a conical pick

Table 3 Modelling scheme for the numerical investigation of rock cutting

Case	Cutting velocity [m/s]	Depth of cut [mm]	Rake angle [°]	Tip angle [°]	Tip wear [%]	Tip shape
A-1 (a-d)	1 / 2.5 / 5 / 10	1	-15	75	-	Conical
A-2 (a-d)	1 / 2.5 / 5 / 10	3	-15	75	-	Conical
A-3 (a-d)	1 / 2.5 / 5 / 10	5	-15	75	-	Conical
A-4 (a-d)	1 / 2.5 / 5 / 10	7	-15	75	-	Conical
A-5 (a-e)	5	1	-37.5 / -30 / 0 / 7.5 / 12.5	75	-	Conical
A-6 (a-e)	5	3	-37.5 / -30 / 0 / 7.5 / 12.5	75	-	Conical
A-7 (a-e)	5	5	-37.5 / -30 / 0 / 7.5 / 12.5	75	-	Conical
A-8 (a-e)	5	7	-37.5 / -30 / 0 / 7.5 / 12.5	75	-	Conical
A-9 (a-c)	5	3	-30	60 / 90 / 105	-	Conical
B-1 (a-d)	5	1	-45	90	0% / 10% / 20% / 50%	Conical
C-1 (a-c)	5	1	-45	90	-	Conical / Ballistic / Rounded

2.2 Rock cutting model setup and modelling scheme

A cutting tool and a base rock model were considered to simulate the rock cutting. As illustrated in Fig. 3, the rake angle (α), tip angle (θ) and depth of cut (Dc) are defined.

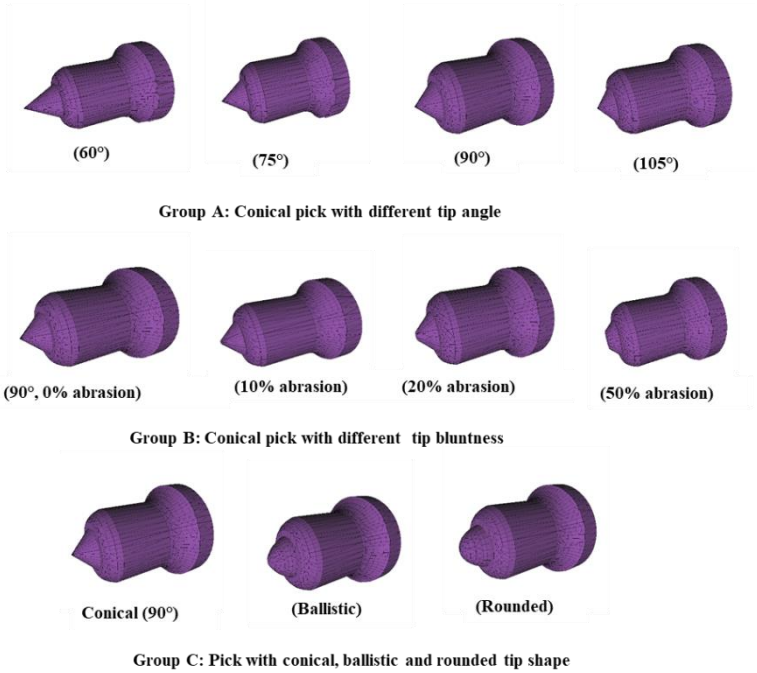

Fig. 4 Picks constructed for the rock cutting simulation

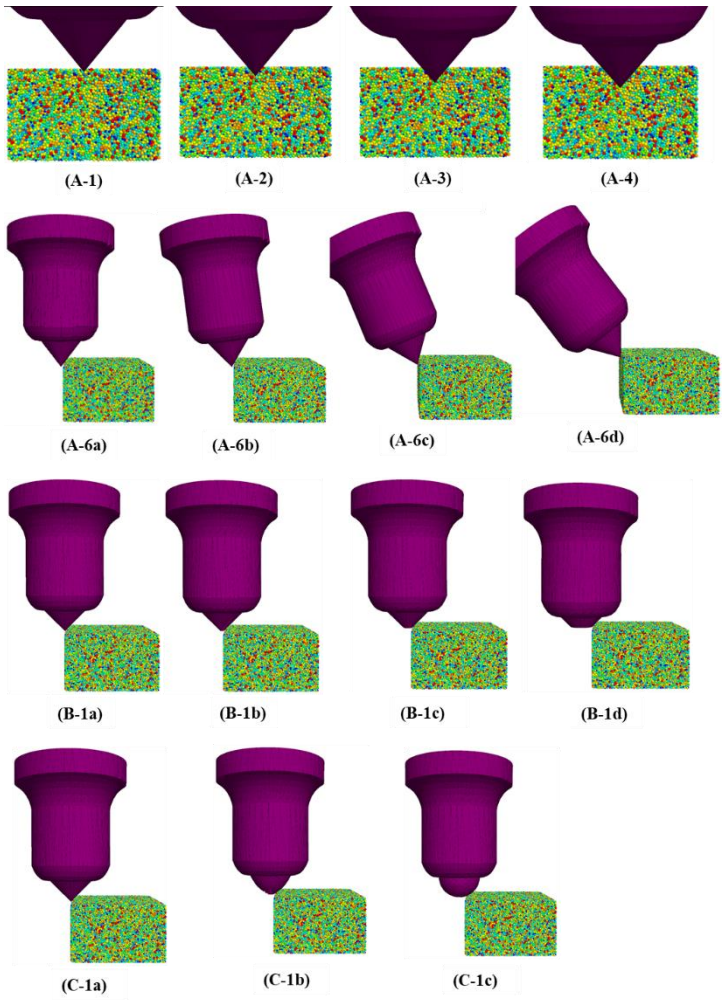

Fig. 5 PFC models for the rock cutting simulation under different operation conditions (Exemplary: A1 - A4 with different cut depths, A6a - A6d with different rake angles, B1a - B1d with different tip abrasions, C1a - C1c with different pick shapes)

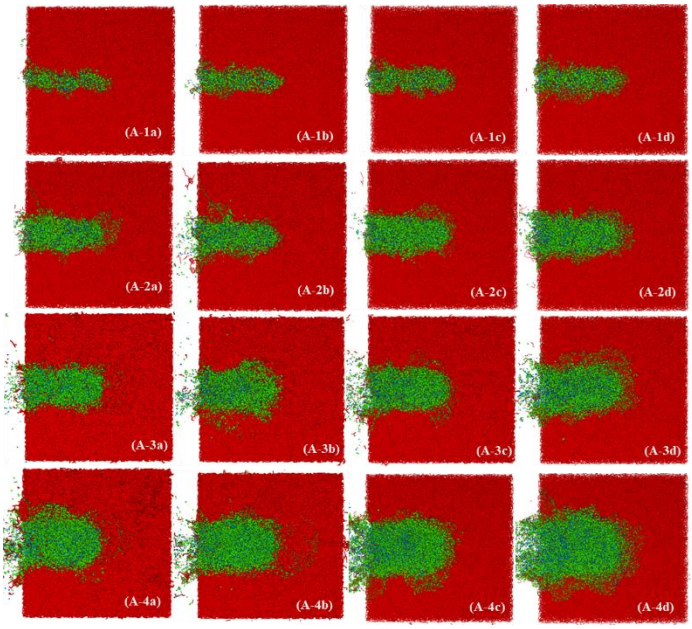

Fig. 6 Crack patterns with cutting velocities of 1 m/s, 2.5 m/s, 5 m/s and 10 m/s and cut depths of 1 mm, 3 mm, 5 mm and 7 mm in the case of 75° tip angel and -15° rake angle (Exemplary: blue circles indicate the cracks in shear, green circles indicate the cracks in tension, red lines indicate the parallel bonds)

Three groups of the cutting tool were constructed (Fig. 4), Group A: conical pick with tip angle of 60°, 75°, 90°, and 105° respectively; Group B: conical pick with tip abrasion (or bluntness) of 0%, 10%, 20%, and 50% respectively; Group C: the pick with conical, ballistic and rounded tip shape. The base rock model has a dimension of 50 mm in length, 50 mm in width and 30 mm in height. The particle radii are generated between 0.4 - 0.6 mm. The rock sample is composed of 134 872 particles.

Fig. 5 illustrates the PFC models for the rock cutting simulation under different operation conditions. The cutter head was moved against the stationary rock sample with the sliding velocities of 1 m/s, 2.5 m/s, 5 m/s and 10 m/s at cut depths of 1 mm, 3 mm, 5 mm and 7 mm, respectively. The cutting tool had a rake angle, α, of -37.5°, -30°, 0° and 7.5°, respectively. During these simulations, the top side and left side of the model were set to free, whereas the other sides were fixed. The cutting tool was moved from left to right over the sample piece for a sliding distance of 25 mm to have a better understanding of the evolution of cutting forces and the identification of crack patterns. Normal and sideway velocities were defined as zero. The micro-parameters were inherited from those calibrated for the sandstone (see Table 1). The mechanical damping was set to 0.1. For each simulation, only one parameter was changed, while the other parameters were kept constant. The detailed modelling scheme is listed in Table 3.

3. Results and discussion

During the rock cutting process, the applied tool force can be decomposed into three orthogonal components: normal force, cutting force and sideway force. The normal force is defined as the force perpendicular to the cutting direction, the cutting force is in line with the cutting direction and the sideway force is lateral to the cutting direction.

Rock fracturing and fragmentation of the sandstone model can be expressed by the detachment of particles due to breakage of the bonds. After the pick interacts with the particles, micro-cracks in forms of tension and shear initiate and propagate from the pick tip, which results in fractures. With ongoing of the pick, more and more bonded particles are detached and removed by it. The forward propagation of cracks leads to the removal of the front particles. Since the cutting force and the number of cracks are the two most important parameters describing the interaction between the tool and rock, the analysis only focused on the resulting cutting force and induced cracks.

3.1 Influence of cutting velocity and depth of cut (cases A1 - A4)

Verhoef (1997) found that the cutting force does not vary much with cutting velocity at lower values, while the influence of cutter velocity on the cutting force is substantial only at higher velocities. Moreover, he concluded that the cutting velocity has a significant influence on the cutting force at a greater cut depth. This conclusion was confirmed by Menezes *et al.* (2014) by conducting rock cutting simulations using FEM-based code. In addition, numerical study of Tan *et al.* (2009) showed that a higher cutting velocity combined with a smaller cut depth can reduce the surface damage of brittle materials, as same as the amount of induced cracks. Experimental investigations have also shown that ductile failure takes place at a small cut depth, whereas brittle failure occurs at a large one (Huang *et al*. 2013). It has also been found that the cutting force and chip size increases with increasing

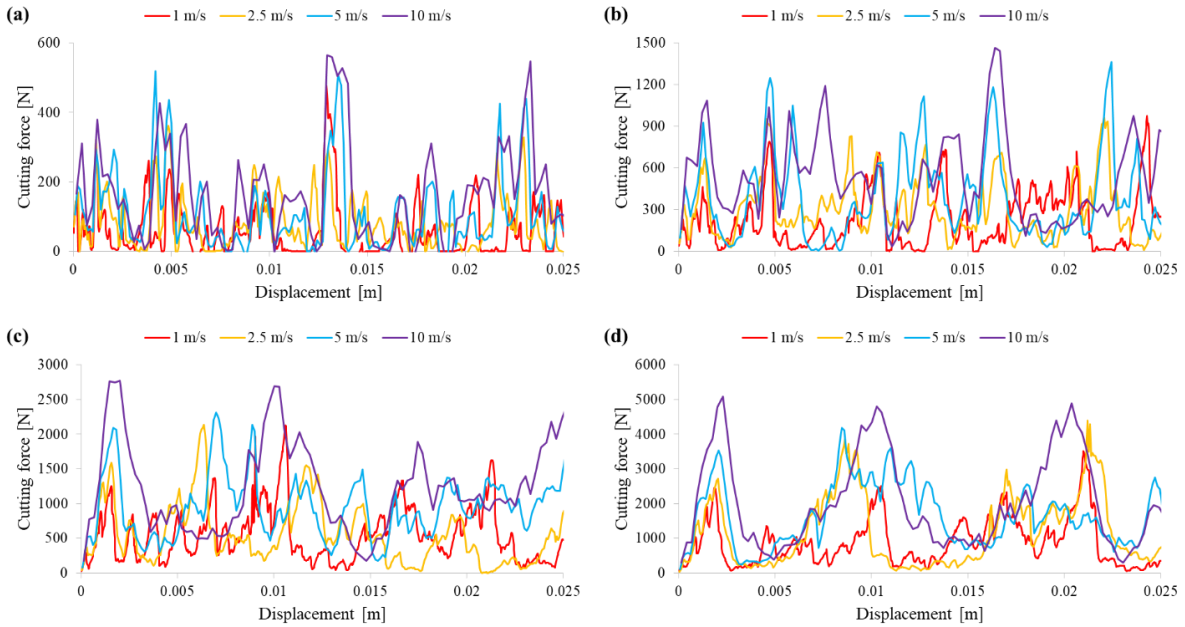

Fig. 7 Evolution of cutting forces with different cutting velocities for the cut depths of (a) 1 mm, (b) 3 mm, (c) 5 mm and (d) 7 mm in the case of 75° tip angle and -15° rake angle

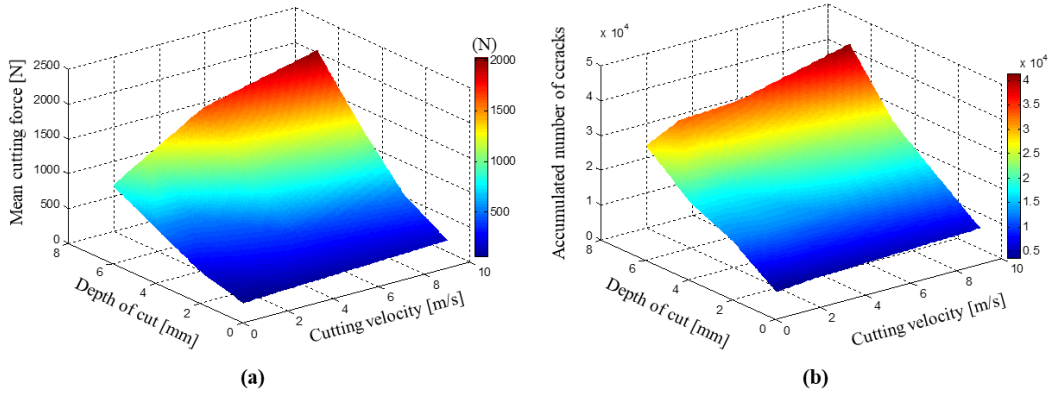

Fig. 8 Variation of (a) mean cutting forces and (b) total accumulated number of cracks versus cutting velocities and cut depths in the case of 75° tip angel and -15° rake angle

depth of cut (Gray *et al.* 1962, Lei *et al.* 2004, Menezes *et al.* 2014).

Rock cutting simulations were conducted by specifying different cutting velocities (1 m/s, 2.5 m/s, 5 m/s and 10 m/s) and depths of the cut (1 mm, 3 mm, 5 mm and 7 mm) on a 75° conical pick for a given rake angle of -15°.

Fig. 6 illustrates the crack patterns at the final state of the simulation related to the cutting velocities and depths. The tensile-induced cracks are visible in green and the shear-induced cracks in blue. It is obvious that the number of tensile cracks is higher than that of shear cracks, which means that the failure mode in the rock cutting is dominant a tensile one. This finding coincides with the rock cutting theory of Nishimatsu (1972). Moreover, it is found that more cracks are induced when the cutting velocity and depth of cut increase. The more the cracks occur, the severer the rock fragments. Fig. 7 shows the cutting forces fluctuating during the cutting process. For a given depth value, the peak cutting force increases with increasing cutting velocity. The increase or decrease of cutting forces can be related to the crack generation. In rock cutting engineering, the mean cutting force is calculated as the average of the recorded force data over the sliding distance. Fig. 8(a) shows the numerically obtained mean cutting force plotted against the corresponding cutting velocity and cut depth. For shallow cutting, the velocity effect on the cutting force is not very obvious, but the influence becomes more and more significant as the depth of cut increases. Fig. 8(b) indicates that the total accumulated number of cracks (defined as the sum of cracks in tension and cracks in shear) increases slightly with increasing cutting velocity at a small depth, and increases significantly with increasing cut depth. Summarized, it can be concluded that a high cutter velocity with a great cut depth enhances the cutting force and increases the amount of cracks compared to a low velocity with a small depth.

3.2 Influence of rake angle (cases A5 - A8)

The rake angle is another main factor affecting the

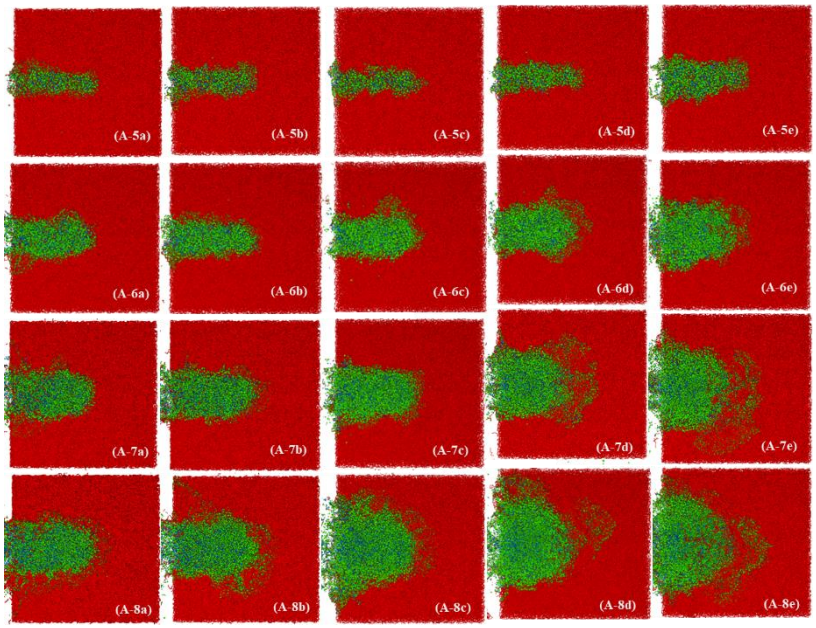

Fig. 9 Crack patterns with rake angles of -37.5°, -30°, 0°, 7.5° and 12.5° and cut depths of 1 mm, 3 mm, 5 mm and 7 mm in the case of 75° tip angle and 5 m/s cutting velocity

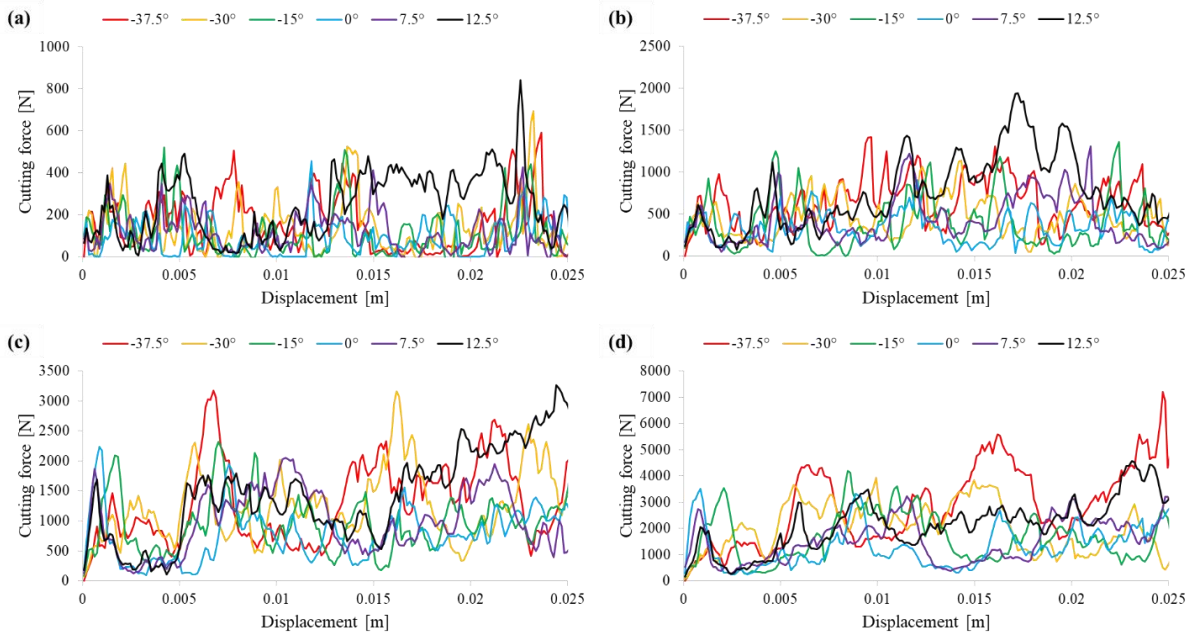

Fig. 10 Evolution of cutting forces with different rake angles for the cut depths of (a) 1 mm, (b) 3 mm, (c) 5 mm and (d) 7 mm in the case of 75° tip angle and 5 m/s cutting velocity

cutting force, crack pattern as well as rock fragmentation. Gray *et al.* (1962) performed a series of cutting tests on limestone with a drag pick at different rake angles ranging from positive to negative values (30°, 15°, 0°, -15° and -30°). They concluded that the tool forces, i.e., normal force and cutting force, increase with decreasing rake angle, especially for rake angles smaller than 0°. Based on the rock cutting tests conducted on limestone and granite at different negative rake angles (0°, -5°, -10°, -15° and -20°), Goektan (1990) found that the cutting force decreases with increased negative rake angle. By performing rock cutting experiments on sandstone and concrete with a drag pick, Guo *et al.* (1992) found that the cutting force increases with the increase of positive rake angles (0°, 7.5° and 15°). Moreover, he concluded that crack propagation along a curved path becomes larger when the rake angle is greater. Lei *et al.* (2004) performed two dimensional numerical simulations of rock cutting on marble with two different rake angles (15° and 25°). Results showed that the resultant cutting force with a rake angle of 25° is also higher than that with 15°.

The rake angle effect on cutting forces and crack patterns was studied with a tip angle of 75° by applying different rake angles ranging from negative to positive

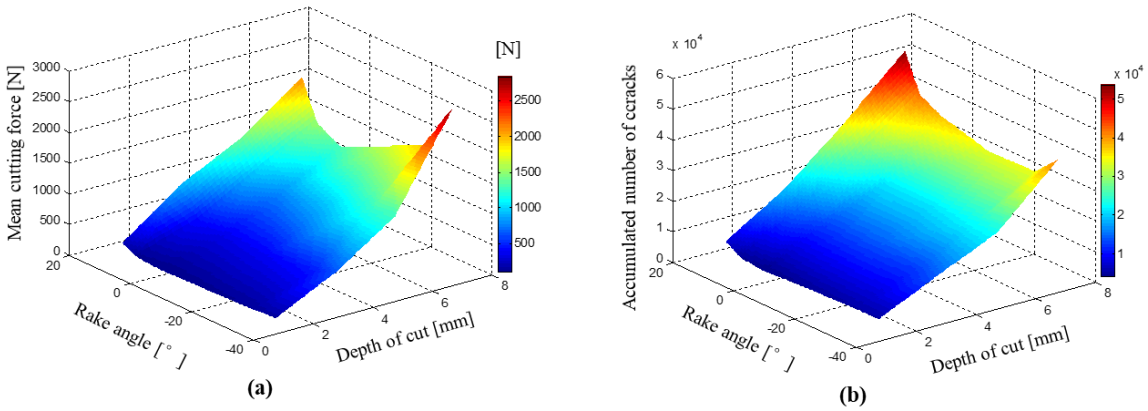

Fig. 11 Variation of (a) mean cutting forces and (b) total accumulated number of cracks versus rake angles and cut depths in the case of 75° tip angle and 5 m/s cutting velocity

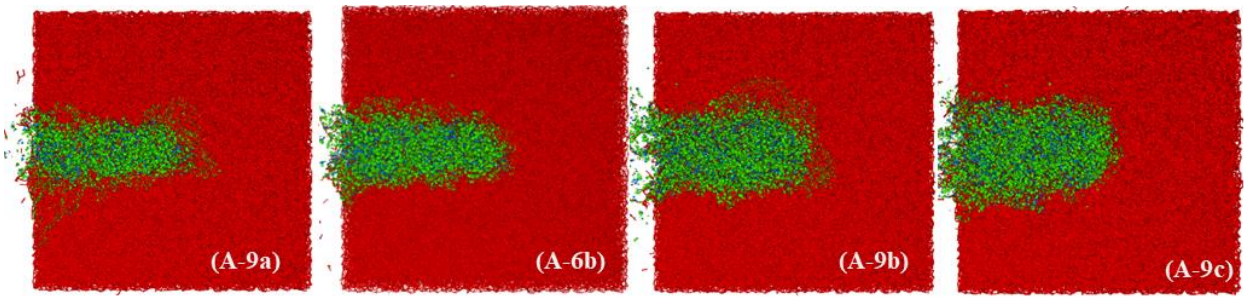

Fig. 12 Crack patterns with tip angles of 60°, 75°, 90° and 105° in the case of -30° rake angle

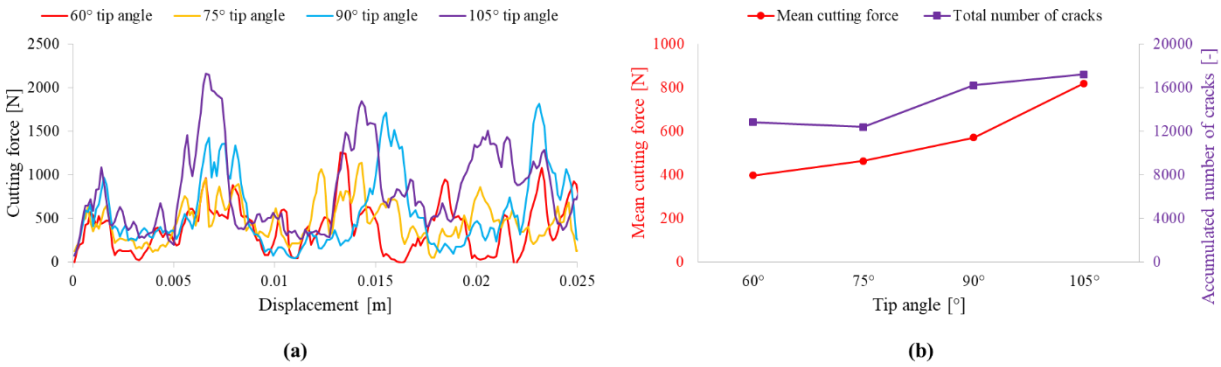

Fig. 13 (a) Evolution of cutting forces with different tip angles; (b) Variation of mean cutting forces and total accumulated number of cracks versus tip angles (rake angle = -30°)

values (-37.5°, -30°, 0°, 7.5° and 12.5°) and with depths of the cut (1 mm, 3 mm, 5 mm and 7 mm), respectively. A constant cutting velocity of 5 m/s was used in the simulations.

Figs. 9 and 10 show the crack patterns and cutting forces correlated with the corresponding rake angles at different cut depths. For a given depth, the force value and amount of cracks are firstly reduced with increasing negative rake angle, and then increased with increasing positive rake angle. For both, negative and positive rake angles, the cutting force becomes more and more sensitive to the increased cut depth, as same as the cracks. In Fig. 11, the mean cutting forces and total induced cracks are related to the rake angles and depths of the cut. For rake angles smaller than 0°, the mean cutting force decreases with increasing negative rake angle, and then increases with increasing positive rake angle. The lowest force value is obtained at the rake angle of 0°. Similarly, the number of accumulated cracks decreases with the increase in negative rake angle and increases with the increase in positive rake angle. Summarized, the rake angle effect on cutting forces is more sensitive for greater depths of the cut and higher cutting velocities, and this finding is also appropriate for the cracking.

3.3 Influence of tip angle (case A9)

In mining industry, tip angles of conical picks are usually designed between 60° and 90° (60° for cutting soft rocks and 90° for cutting hard rocks), and 75°-80° are the most commonly manufactured tip angles (Bilgin *et al.* 2006). Experimental study of tip angles affecting the cutting

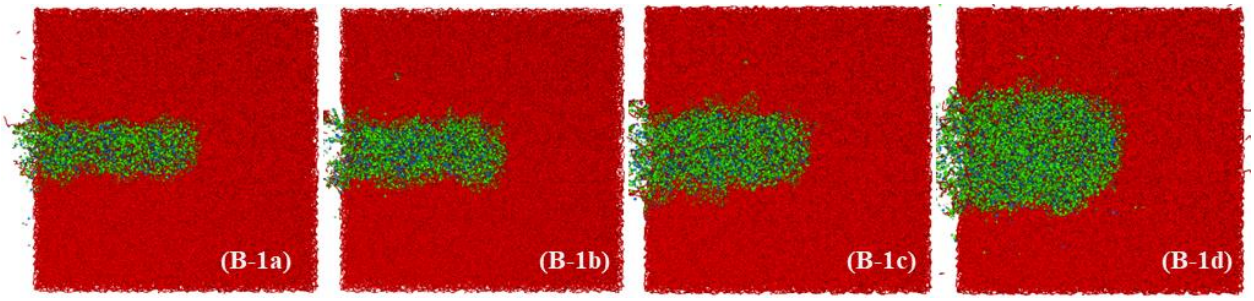

Fig. 14 Crack patterns with tip abrasions of 0%, 10%, 20% and 50% in the case of 90° tip angle

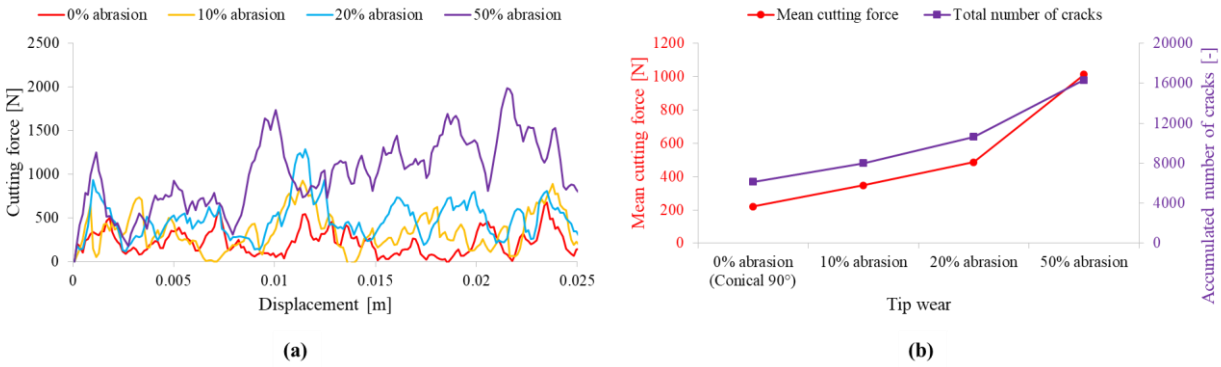

Fig. 15 (a) Evolution of cutting forces with different tip abrasions and (b) Variation of mean cutting forces and total accumulated number of cracks versus tip abrasions (tip angle = 90°)

forces was performed by Sarwary and Hagan (2016). In their work, four different tip angles (70°, 90°, 100° and 110°) were tested on two types of rock (sandstone and limestone). Results showed that the cutting force increases with the increase in tip angle. However, the rake angles for the corresponding tip angles used for their tests are quite different from each another: with the value of 10° rake angle for 70° tip angle, 0° rake angle for 90° tip angle, -5° rake angle for 100° tip angle and -10° rake angle for 110° tip angle.

To evaluate the efficiency of different cutter heads, or in other words, to design an optimal head for cutting rocks, it is necessary to examine the dependency of cutting forces and crack formations on the tip angle. In this paper, besides the 75° tip angle, three additional tip angles of 60°, 90° and 105° were constructed for the numerical investigation. In the simulations, the rake angle was fixed at -30° in order to exclude its effect on the simulation result.

Figs. 12 and 13 indicate that the tip angle has a significant influence on the cutting force, crack evolution and rock fragmentation. Fig. 12 illustrates the final state of the fragmentation of sandstone model. It is obvious that the fragmentation area of model increases with increasing tip angle. A larger tip angle generates more cracks, but the applied cutting force is also higher on it, and vice versa (see Fig. 13).

3.4 Influence of tip wear (case B)

A clear difference between the actual laboratory experiments and numerical simulations of rock cutting is that the wear on the cutting tool is not considered in the simulation. Therefore, a deviation between the numerical and experimental results can be expected. Experimental study of Guo *et al.* (1992) showed that the blunting of cutting tools results in a higher cutting forces and in a poor cutting efficiency. Su and Akcin (2011) stated: when a worn pick is used for the simulation, the resultant force will inevitably be increased. Van Wyk *et al.* (2014) emphasized that only a small amount of wear on the cutters can affect a cutting process to a great extent and make the cutting more difficult.

The influence of tool abrasion on cutting forces and crack patterns was investigated by chamfering a 90° conical pick artificially with three different bluntness ratios of 10%, 20% and 50%. In the simulations, each pick was set orthogonal (90°) to the sample model to exclude the influence of the rake angle on the numerical result. The cutting velocity was fixed at 5 m/s and the depth of cut was set to 1 mm.

Figs. 14 and 15 show the variation of rock fragmentation, cutting forces and accumulated number of cracks with diverse wear flats. It is not difficult to see that the cutting force increases with increasing tip wear. This is caused by the friction coefficient at the interface between the worn tip and the sample surface, which cannot be neglected in varying the rake angles between the tool and rock in the course of the cutting process, and therefore the stress distribution on the cutting tool as well as the cutting force during the rock cutting. It is concluded that rock cutting with sharp tips obviously requires less force than with blunt tips. Moreover, it is found that the increase of cutting force is not linear with the tip wear. An exponential relationship can better describe this relation. This in fact means an increased demand in power and makes the cutting process inefficient. In addition, looking at the rock

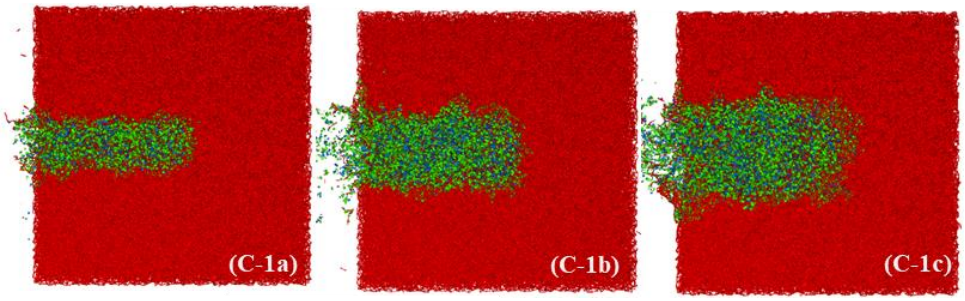

Fig. 16 Crack patterns with conical (90°), ballistic and rounded tip shapes

properties of sandstone, numerical simulations of rock

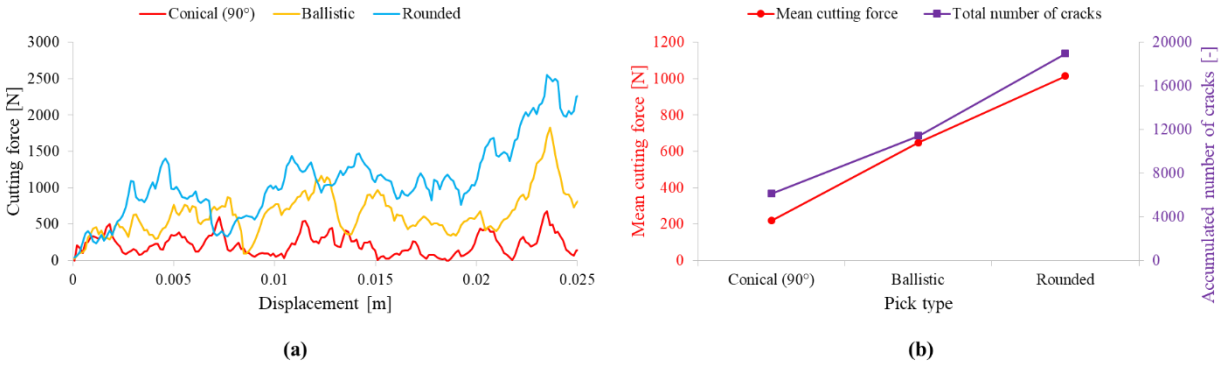

Fig. 17 (a) Evolution of cutting forces with different tip shapes and (b) Variation of mean cutting forces and total accumulated number of cracks versus tip shapes

fracturing during the simulated cutting process, it is concluded that the abraded pick can induce more cracks than that without abrasion, and exponential relationship can also be identified.

3.5 Influence of tip shape (case C)

A large variety of picks has been designed to excavate rocks with different strength and abrasivity properties. In general, conical picks are often used to excavate softer and lower abrasive rocks, but the wear on it is also higher. Ballistic picks are used for hard rocks with low abrasivity, and its abrasion is moderate. Rounded picks can be used to excavate rocks with higher strength and greater abrasive potential due to lower abrasion (Thuro, 1996).

To examine the dependency of cutting forces and crack patterns on the pick type, rock cuttings were simulated with conical, ballistic and rounded tip shape, respectively, under the same testing conditions (cutting velocity = 5 m/s, depth of cut = 1 mm, rake angle = -45°).

In Figs. 16 and 17, the cutting forces and number of cracks are related to the three tip shapes. It is found that the greatest cutting force is required for the rounded pick, followed by the ballistic pick, and then by the conical pick. The rounded pick causes the most cracks, while the conical pick produces the least amount of cracks. This finding confirms the statement of Thuro (1996).

4. Conclusions

In this paper, based on the mineralogical-mechanical cutting were conducted using PFC^{3D}, in which the bonded particle model associated with the parallel bonds was used. The influence of cutting parameters and tool geometries on the cutting force and rock fracturing and fragmentation was studied. The following conclusions can be drawn:

• The cutting velocity associated with depth of cut have a significant influence on cutting forces and crack patterns. Especially at a greater cut depth, the increase of cutting velocity leads to an enhancement of cutting forces.

• The rake angle effect on the variation of cutting forces reveals that the resulting cutting force firstly decreases with increased negative rake angle, and subsequently increases with increased positive rake angle. The lowest force value is obtained in the case of that the rake angle equals to 0°.

• The cutter geometry, especially the tip angle, is one of the major factors affecting the resultant cutting force. A larger tip angle enhances the requirement of cutting force and induces more cracks than a smaller tip angle.

• The wear on the cutter tip can affect the cutting force significantly. Cutter heads with blunt tip obviously require more force than with sharp tip.

• For a given rock material, rounded pick can cause the most cracks, but the required force on it is also highest, while conical pick produces the least cracks and needs the lowest cutting force.

It should be noticed that, besides the cutting parameters and tool geometry, as discussed in the present paper, the applied tool force depends also on the rock types with respect to their mechanical properties. It can be envisaged that the cutting force is comparatively different, or more exactly, is higher for basalt or granite due to its higher strength compared to the sandstone, and the induced cracks

can also be reduced in such strong rocks. This effecting factor will be studied by simulating different rock materials and under dynamic load conditions in further works (Dang *et al.*, 2019; Duan *et al.*, 2019). The DEM modelling can be used instead of the experimental works, if an actual rock cutting experiment is more expensive and time-consuming, as well as a 'trial-and-error' study should be conducted for the rock excavations in more complex geological situations.

Acknowledgments

This work was supported by the National Nature Science Foundation of China (51904359), Natural Science Foundation of Guangdong (2020A151501528) and the Fundamental Research Funds for the Central Universities (19lgzd41). The first author would like to thank the Chinese Scholarship Council (CSC) (201408080085) for its financial support. Special thanks to Mr. Qiaofeng Ni and Mr. Mingzhi Zheng at TU Bergakademie Freiberg in constructing the cutting tools.

References

Balci, C. and Bilgin, N. (2007), "Correlative study of linear small and full-scale rock cutting tests to select mechanized excavation machines", *Int. J. Rock Mech. Min. Sci.*, **44**(3), 468-476. https://doi.org/10.1016/j.ijrmms.2006.09.001.

Bilgin, N., Demircin, M.A., Copur, H., Balci, C., Tuncdemir, H. and Akcin, N. (2006), "Dominant rock properties affecting the performance of conical picks and the comparison of some experimental and theoretical results", *Int. J. Rock Mech. Min. Sci.*, **43**(1), 139-156. https://doi.org/10.1016/j.ijrmms.2005.04.009.

Chang, S., Lee, C., Kang, T.H., Ha, T. and Choi, S.W. (2017), "Effect of hardfacing on wear reduction of pick cutters under mixed rock conditions", *Geomech. Eng.*, **13**(1), 141-159. https://doi.org/10.12989/gae.2017.13.1.141.

Cundall, P.A. (1971), "A computer model for simulating progressive large scale movements in blocky rock system", *Proceeding of the Symposium of the International Society of Rock Mechanics*, Nancy, France, September.

Cundall, P.A. (1988), "Formulation of a three-dimensional distinct element model – Part I. A scheme to detect and represent contacts in a system composed of many polyhedral blocks", *Int. J. Rock Mech. Min. Sci. Geomech.*, **25**(3), 107-116. https://doi.org/10.1016/01489062(88)91214-4.

Cundall, P.A. and Hart, R. (1992), "Numerical modeling of discontinua", *Eng. Comput.*, **9**, 101-113. https://doi.org/10.1016/B978-0-08-040615-2.50015-0.

Dang, W., Konietzky, H. and Li, X. (2019), "Frictional responses of concrete-to-concrete bedding planes under complex loading conditions", *Geomech. Eng.*, **17**(3), 253-259. https://doi.org/10.12989/gae.2019.17.3.253.

Ding, X., Zhang, L., Zhu, H. and Zhang, Q. (2014), "Effect of model scale and particle size distribution on PFC3D simulation results", *Rock Mech. Rock Eng.*, **47**(6), 2139-2156. https://10.1007/s00603-013-0533-1.

Duan, K., Ji, Y., Wu, W. and Kwok, C.Y. (2019), "Unloading-induced failure of brittle rock and implications for excavation-induced strain burst", *Tunn. Undergr. Sp. Technol.*, **84**, 495-506. https://doi.org/10.1016/j.tust.2018.11.012.

Evans, I. (1984), "A theory of the cutting force of point-attack picks", *Int. J. Min. Eng.*, **2**(1), 63-71. https://doi.org/10.1007/bf00880858.

Fowell, R.J., Richardson, G. and Gollick, M.J. (1994), "Prediction of boom tunneling machine excavation rates", *Proceeding of the 1st North American Rock Mechanics Symposium*, Austin, Texas, U.S.A., June.

Goektan, R.M. (1990), "Effect of cutter pick rake angle on the failure pattern of high-strength rocks", *Min. Sci. Technol.*, **11**(3), 281-285. https://doi.org/10.1016/0167-9031(90)90981-w.

Gray, K.E., Armstrong, F. and Gatlin, C. (1962), "Two-dimensional study of rock breakage in drag-bit drilling at atmospheric pressure", *J. Petrol. Technol.*, **14**(1), 93-98. https://doi.org/10.2118/164-pa.

Guo, H., Aziz, N.I. and Schmidt, L.C. (1992), "Rock cutting study using linear elastic fracture mechanics", *Eng. Fract. Mech.*, **41**(5), 771-778. https://doi.org/10.1016/0013-7944(92)90159-c.

Hart, R.D., Cundall, P.A. and Lemos, J. (1988), "Formulation of a three-dimensional distinct element model – Part II. Mechanical calculations for motion and interaction of a system composed of many polyhedral blocks", *Int. J. Rock Mech. Min. Sci. Geomech.*, **25**(3), 117-125. https://doi.org/10.1016/0148-9062(88)92294-2.

Huang, H., Lecampion, B. and Detournay, E. (2013), "Discrete element modeling of tool-rock interaction I: Rock cutting", *Int. J. Rock Mech. Min. Sci. Geomech.*, **37**, 1913-1929. https://doi.org/10.1002/nag.2113.

Hurt, K.G. and MacAndrew, K.M. (1985), "Cutting efficiency and life of rock cutting picks", *Min. Sci. Tech.*, **2**, 139-151. https://doi.org/10.1016/s0167-9031(85)90357-3.

Itasca (2016), *PFC^{3D} Version 5.0*, Itasca Consulting Group, Minneapolis, Minnesota, U.S.A.

Jeong, H. and Jeon, S. (2018), "Characteristic of size distribution of rock chip produced by rock cutting with a pick cutter", *Geomech. Eng.*, **15**(3), 811-822. https://doi.org/10.12989/gae.2018.15.3.811.

Kwok, C., Duan, K. and Pierce, M. (2019) "Modeling hydraulic fracturing in jointed shale formation with the use of fully coupled discrete element method", *Acta Geotech.*, **15**(1), 245-264. https://doi.org/10.1007/s11440-019-00858-y.

Lei, S., Kaitkay, P. and Shen, X. (2014), "Simulation of rock cutting using distinct element method – PFC2D", *Proceeding of the 2nd International PFC Symposium*, Kyoto, Japan, October.

Lei, S.T. and Kaitkay, P. (2003), "Distinct element modeling of rock cutting under hydrostatic pressure", *Key Eng. Mater.*, **250**, 110-117. https://doi.org/10.4028/www.scientific.net/kem.250.110.

Li, Y., Sun, S. and Tang, C. (2019), "Analytical prediction of the shear behaviour of rock joints with quantified waviness and unevenness through wavelet analysis", *Rock Mech. Rock Eng.*, **52**, 1-13. https://doi.org/10.1007/s00603-019-01817-5.

Lunow, C. and Konietzky, H. (2012), "Two dimensional and three dimensional simulation of rock cutting processes", *Proceedings of the Freiberg High-Pressure Symposium*, Freiberg, Germany, October.

McFeat-Smith, I. and Fowell, R.J. (1977), "Correlation of rock properties and the cutting performance of tunneling machines", *Proceeding of the Conference on Rock Engineering*, Newcastle upon Tyne, U.K.

Menezes, P.L., Lovell, M.R., Avdeev, I.V. and Fred Higgs III, C. (2014), "Studies on the formation of discontinuous rock fragments during cutting operation", *Int. J. Rock Mech. Min. Sci.*, **71**, 131-142. https://doi.org/10.1016/j.ijrmms.2014.03.019.

Nishimatsu, Y. (1972), "The mechanics of rock cutting", *Int. J. Rock Mech. Min. Sci. Geomech. Abstr.*, **9**(2), 261-270. https://doi.org/10.1016/0148-9062(72)90027-7.

Potyondy, D.O. and Cundall, P.A. (2004), "A bonded-particle model for rock", *Int. J. Rock Mech. Min. Sci.*, **41**(8), 1329-1364. https://doi.org/10.1016/j.ijrmms.2004.09.011.

Rojek, J., Onate, E., Labra, C. and Kargl, H. (2011), "Discrete element simulation of rock cutting", *Int. J. Rock Mech. Min. Sci.*, **48**(6), 996-1010. https://doi.org/10.1016/j.ijrmms.2010.08.012.

Sarwary, E. and Hagan, P.C. (2016), "The effect of changes in tool tip angle on the cutting performance of a pointed pick", *Min. Technol.*, **125**(3), 184-190. https://doi.org/10.1080/14749009.2016.1159056.

Shang, J., Zhao, Z. and Ma, S. (2018), "On the shear failure of incipient rock discontinuities under CNL and CNS boundary conditions: insights from DEM modeling", *Eng. Geol.*, **234**, 153-166. https://doi.org/10.1016/j.enggeo.2018.01.012.

Shang J. (2020), "Rupture of veined granite in polyaxial compression: Insights from three-dimensional discrete element method modelling", *J. Geophys. Res. Solid Earth*. https://doi.org/10.1029/2019JB019052.

Shang J., Zhao Z., Hu J. and Handley K. (2018) "3D particle-based DEM investigation into the shear behaviour of incipient rock joints with various geometries of rock bridges", *Rock Mech. Rock Eng.*, **51**(11), 3563-3584. https://doi.org/10.1007/s00603-018-1531-0.

Su, O. and Akcin, N.A. (2011), "Numerical simulation of rock cutting using the discrete element method", *Int. J. Rock Mech. Min. Sci.*, **48**, 434-442. https://doi.org/10.1016/j.ijrmms.2010.08.012.

Tan, Y.Q., Yang, D.M. and Sheng, Y. (2009), "Discrete element method (DEM) modeling of fracture and damage in the machining process of polycrystalline SiC", *J. Eur. Ceramic Soc.*, **29**(6), 1029-1037. https://doi.org/10.1016/j.jeurceramsoc.2008.07.060.

Thuro, K. (1996), "Bohrbarkeit beim konventionellen Sprengvortrieb. Geologisch-felsmechanische Untersuchungen anhand sieben ausgewählter Tunnelprojekte", Ph.D. Dissertation, Technische Universität München, München, Germany.

Van Wyk, G., Els, D.N.J., Akdogan, G., Bradshaw, S.M. and Sacks, N. (2014), "Discrete element simulation of tribological interactions in rock cutting", *Int. J. Rock Mech. Min. Sci.*, **65**, 8-19. https://doi.org/10.1016/j.jeurceramsoc.2008.07.060.

Verhoef, P.N.W. (1997), "Wear of rock cutting tools: implications for the site investigation of rock dredging projects", Ph.D. Dissertation, Technical University Delft, Delft, The Netherlands.

Wang, S., Huang, L. and Li, X. (2020), "Analysis of rockburst triggered by hard rock fragmentation using a conical pick under high uniaxial stress", *Tunn. Undergr. Sp. Technol.*, **96**, 103195. https://doi.org/10.1016/j.tust.2019.103195.

Yang, X.Q., Zhang, L.J. and Ji, X.M. (2013), "Strength characteristics of transversely isotropic rock materials", *Geomech. Eng.*, **15**(1), 71-86. https://doi.org/10.12989/gae.2013.5.1.071.

Zhu, X., Liu, W. and Lv, Y. (2017), "The investigation of rock cutting simulation based on discrete element method", *Geomech. Eng.*, **13**(6), 977-995. https://doi.org/10.12989/gae.2017.13.6.977.